

Cyclopalladation of the Indole Ring in Palladium(II) Complexes of 2N1O-Donor Ligands and Its Dependence on the O-Donor Properties

Yuichi Shimazaki,^{*,†} Minoru Tashiro,[‡] Takeshi Motoyama,[‡] Satoshi Iwatsuki,[§] Tatsuo Yajima,[‡] Yasuo Nakabayashi,[‡] Yoshinori Naruta,[†] and Osamu Yamauchi^{*,‡}

Institute for Materials Chemistry and Engineering, Kyushu University, Higashi-ku, Fukuoka 812-8581, Japan, Unit of Chemistry, Faculty of Engineering, Kansai University, Suita, Osaka 564-8680, Japan, and Department of Chemistry, Graduate School of Science and Engineering, Waseda University, Okubo, Shinjuku-ku, Tokyo 169-8555, Japan

Received April 1, 2005

Synthetic, structural, spectroscopic, and kinetic studies have been carried out on the Pd(II) complexes of new 2N1O-donor ligands containing a pendent indole, 3-(*N*-2-pyridylmethyl-*N*-2-hydroxy-5-methoxybenzylamino)ethylindole (HMeO-iepp), 3-(*N*-2-pyridylmethyl-*N*-2-hydroxy-5-nitrobenzylamino)ethylindole (HNO₂-iepp), and (*N*-2-pyridylmethyl-3-indolylethylamino)acetic acid (Hiepc) (H denotes a dissociable proton). [Pd(MeO-iepp)Cl] (**2**), [Pd(NO₂-iepp)Cl] (**3**), and [Pd(iiepc)Cl] (**4**) were prepared and revealed by X-ray analysis to have a pyridine nitrogen, an amine nitrogen, a phenolate or carboxylate oxygen, and a chloride ion in the coordination plane. UV absorption and ¹H NMR spectral changes indicated that all the complexes could be converted to the indole-binding complexes where the O donor was replaced by the indole C2 atom by cyclopalladation in DMSO or DMF in the temperature range of 40–60 °C. Formation of the indole-binding complex species obeyed the first-order kinetics, from which the activation parameters were estimated. The formation rate was dependent on the properties of the O-donor group, a lower pK_a value of its conjugate acid causing faster conversion to the indole-binding species in the order **2** (methoxyphenolate) < **3** (nitrophenolate) < **4** (carboxylate). On the other hand, the ratio of the indole-binding complex to the O-donor complex as a result of the conversion was greater for the complexes with a higher pK_a value of the ligand OH group, the order being **2** > **3** > **4**.

Introduction

Tryptophan plays important roles in proteins and chemical systems, because of the unique properties of the indole ring.^{1–3} As the most hydrophobic amino acid among the amino acids from protein sources,⁴ tryptophan is often found at or near catalytic and molecular recognition sites. The indole ring of tryptophan sometimes forms stacks with the

side chains of tyrosine and phenylalanine and is reported to be involved in electron tunneling pathways in electron carriers and redox enzymes.^{5,6} Formation of the indolyl radical in proteins has been established for the intermediate, compound I, formed in the course of the catalytic reaction of cytochrome *c* peroxidase (CcP).^{7–11} Indolyl radical formation is possible with systems such as modified azurins, where the photogenerated tryptophan radical has been observed by Gray et al.¹²

* To whom correspondence should be addressed. E-mail: yshima@ms.ifoc.kyushu-u.ac.jp (Y.S.); osamuy@ipcku.kansai-u.ac.jp (O.Y.).

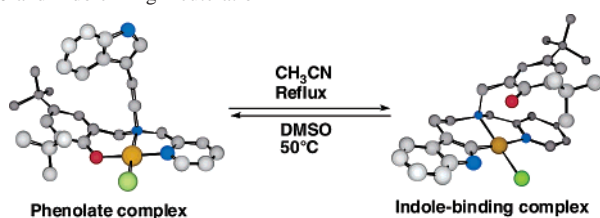
[†] Kyushu University.

[‡] Kansai University.

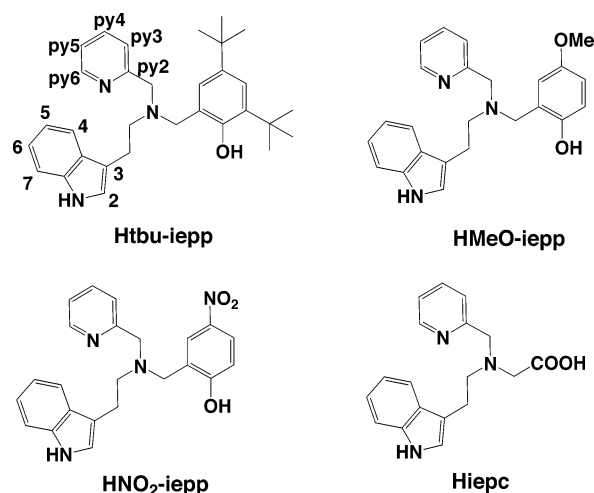
[§] Waseda University.

- (1) (a) Burley, S. K.; Petsko, G. A. *Science* **1985**, 229, 23–28. (b) Burley, S. K.; Petsko, G. A. *Adv. Protein Chem.* **1988**, 39, 125–189. (c) Burley, S. K.; Petsko, G. A. *J. Am. Chem. Soc.* **1986**, 108, 7995–8001. (d) Serrano, L.; Bycroft, M.; Fersht, A. R. *J. Mol. Biol.* **1991**, 218, 465–475. (e) Hunter, C. A.; Singh, J.; Thornton, J. M. *J. Mol. Biol.* **1991**, 218, 837–846.
- (2) Branden, C.; Tooze, J. *Introduction to Protein Structure*, 2nd ed.; Garland Publishing: New York, 1998.
- (3) Meyer, E. A.; Castellano, R. K.; Diederich, F. *Angew. Chem., Int. Ed.* **2003**, 42, 1210–1250.
- (4) Nozaki, Y.; Tanford, C. *J. Biol. Chem.* **1971**, 246, 2211–2217.

- (5) Nordlund, P.; Eklund, H. *J. Mol. Biol.* **1993**, 232, 123–164.
- (6) Pelletier, H.; Kraut, J. *Science* **1992**, 258, 1748–1755.
- (7) Stubbe, J.; van der Donk, W. A. *Chem. Rev.* **1998**, 98, 705–762.
- (8) Isied, S. S. *Met. Ions Biol. Syst.* **1991**, 27, 1–56.
- (9) Nocek, J. M.; Zhou, J. S.; de Frost, S.; Priyadarshy, S.; Beratan, D. N.; Onuchic, J. N.; Hoffman, B. M. *Chem. Rev.* **1996**, 86, 2359–2489.
- (10) Sivaraja, M.; Goodin, D. B.; Smith, M.; Hoffman, B. M. *Science* **1989**, 245, 738–740.
- (11) Poulos, T. L.; Fenna, R. E. *Met. Ions Biol. Syst.* **1994**, 30, 25–75.
- (12) Di Bilio, A. J.; Crane, B. R.; Wehbi, W. A.; Kiser, C. N.; Abu-Omar, M. M.; Carlos, R. M.; Richards, J. H.; Winkler, J. R.; Gray, H. B. *J. Am. Chem. Soc.* **2001**, 123, 3181–3182.

Scheme 1. Interconversion between [Pd(tbu-iepp)Cl] Isomers **1a** and **1b** and Indole Ring Deuteration¹⁸

Although no metal–indole nitrogen bonds are known for biological systems, various modes of indole coordination in transition-metal complexes^{13–18} and π – π interaction with a metal-coordinated aromatic nitrogen ligand^{19–21} have been reported for chemical systems. The Cu(I) complexes of tripodal ligands having an indole moiety in place of one of the coordinating groups were found to have a Cu(I)–(C2=C3) η^2 bond to form a tetrahedral structure.¹³ The indole nitrogen atom of alkylindoles coordinates to Pd(II) as an imine nitrogen of tautomeric 3*H*-indole where the pyrrole hydrogen atom is bound at the C3 atom.¹⁴ Indole-3-acetate (IA) reacts with Pd(II) in the 3*H*-indole form in the presence of pyridine (py) to give a dimeric complex, [Pd₂(IA)₂(py)₂], where Pd(II) binds with the deprotonated C3 and carboxylate oxygen atoms of IA in addition to the imine nitrogen to form a spiro ring.¹⁵ Pd(II)–indole C2 bonding was also reported to occur as a result of cyclopalladation.¹⁷ On the other hand, the Pd(II) and Pt(II) complexes as artificial peptidases developed by Kostić et al. recognize the indole moiety by their high affinity for the indole ring and cleave the adjacent amide or peptide bond specifically.¹⁶ Very recently, we reported some Pd(II) complexes of 2N1O-donor ligands with a pendent indole moiety (Scheme 1), which were found to be interconvertible between the Pd(II)–phenolato(O) and Pd(II)–indole(C2) complexes with a 2N1O1Cl and a 2N1C1Cl donor set, respectively. One-electron oxidation of the Pd(II)–indole(C2) complex yielded the corresponding Pd(II)–indole π -cation radical species.¹⁸ The Pd(II)–indole bonding was formed under thermodynamically controlled conditions in CH₃CN and CH₂Cl₂/CH₃CN. However, the interconversion or formation of the Pd(II)–indole σ bonding was found to be limited by factors such as the distance

**Figure 1.** Structures of ligands.

between the indole ring and the Pd center, the existence of the phenol moiety, and the unsubstituted indole NH moiety.

We carried out crystallographic, spectroscopic, kinetic, and mechanistic studies on the interconversion of the Pd(II) coordination structures of various 2N1O donor ligands containing an indole ring (Figure 1), to gain further insight into the formation of the Pd(II)–indole bond. Especially, we focused on the function of the phenol moiety and prepared a series of the indole-containing ligands with a substituted phenol moiety or a carboxylic acid. Our findings indicate a versatile nature of the indole ring, which may suggest possibilities of tryptophan as a functional unit in biological systems.

Experimental Section

Materials. Sodium cyanoborohydride was obtained from Tokyo Kasei, triethylamine was from Wako, and PdCl₂ was from Aldrich. All the chemicals used were of the highest grade available and were further purified whenever necessary.²² Solvents were purified before use by standard methods.²² DMSO-*d*₆ was purchased from Cambridge Isotope Laboratory. The synthesis of [*N*-2-pyridylmethyl-*N*-2-hydroxy-3,5-di(*tert*-butyl)benzylamino]methylindole (Htbu-iepp) has been reported previously.¹⁸

3-(*N*-2-Pyridylmethyl-*N*-2-hydroxy-5-methoxybenzylamino)-ethylindole (HMeO-iepp). To a solution of 2-hydroxy-5-methoxybenzaldehyde (1.52 g, 10 mmol) and 3-(*N*-2-pyridylmethylamino)-ethylindole^{23,24} (2.6 g, 10 mmol) in methanol (50 mL) was carefully added sodium cyanoborohydride (0.63 g, 10 mmol). The reaction mixture was then stirred for 24 h at room temperature, acidified by addition of concentrated HCl, and evaporated almost to dryness under a reduced pressure. The residue was dissolved in saturated aqueous Na₂CO₃ (50 mL) and extracted with CHCl₃. The combined extracts were dried over Na₂SO₄ and evaporated almost to dryness under reduced pressure to give a white powder. Yield: 2.44 g (63%). ¹H NMR (400 MHz, CDCl₃): δ (vs TMS) 8.52 (d, 1H), 7.94 (s, 1H), 7.51 (t, 1H), 7.34 (d, 1H), 7.30 (d, 1H), 7.13 (m, 3H), 6.99 (t, 1H), 6.94 (d, 1H), 6.73 (m, 2H), 6.59 (d, 1H), 3.87 (s, 2H), 3.85 (s, 2H), 3.72 (s, 3H), 3.01 (m, 2H), 2.92 (m, 2H).

(22) Perrin, D. D.; Armarego, W. L. F.; Perrin, D. R. *Purification of Laboratory Chemicals*; Pergamon Press: Elmsford, NY, 1966.

(23) Yajima, T.; Shimazaki, Y.; Ishigami, N.; Odani, A.; Yamauchi, O. *Inorg. Chim. Acta* **2002**, 337, 193–202.

(24) Shimazaki, Y.; Nogami, T.; Tani, F.; Odani, A.; Yamauchi, O. *Angew. Chem., Int. Ed.* **2001**, 40, 3859–3862.

(13) Shimazaki, Y.; Yokoyama, H.; Yamauchi, O. *Angew. Chem., Int. Ed.* **1999**, 38, 2401–2403.

(14) Yamauchi, O.; Takani, M.; Toyoda, K.; Masuda, H. *Inorg. Chem.* **1990**, 29, 1856–1860.

(15) Takani, M.; Masuda, H.; Yamauchi, O. *Inorg. Chim. Acta* **1995**, 235, 367–374.

(16) (a) Kaminskaia, N. V.; Johnson, T. W.; Kostić, N. M. *J. Am. Chem. Soc.* **1999**, 121, 8663–8664. (b) Kaminskaia, N. V.; Ullmann, G. M.; Fulton, D. B.; Kostić, N. M. *Inorg. Chem.* **2000**, 39, 5004–5013. (c) Kaminskaia, N. V.; Kostić, N. M. *Inorg. Chem.* **2001**, 40, 2368–2377. (d) Milović, N. M.; Kostić, N. M. *Met. Ions Biol. Syst.* **2001**, 38, 145–186.

(17) Robson, R. *Inorg. Chim. Acta* **1982**, 57, 71–77.

(18) Motoyama, T.; Shimazaki, Y.; Yajima, T.; Nakabayashi, Y.; Naruta, Y.; Yamauchi, O. *J. Am. Chem. Soc.* **2004**, 126, 7378–7385.

(19) (a) Fischer, B. E.; Sigel, H. *J. Am. Chem. Soc.* **1980**, 102, 2998–3008. (b) Guogang, L.; Sigel, H. *Z. Naturforsch.* **1989**, 44b, 1555–1566.

(20) Yamauchi, O.; Odani, A.; Hirota, S. *Bull. Chem. Soc. Jpn.* **2001**, 74, 1525–1545.

(21) Yamauchi, O.; Odani, A.; Takani, M. *J. Chem. Soc., Dalton, Trans.* **2002**, 3411–3421 and references therein.

Table 1. Crystallographic Data

	2	3	4
formula	PdC ₂₄ H ₂₄ N ₃ O ₂ Cl	PdC ₂₃ H ₂₁ N ₄ O ₃ Cl	PdC ₁₈ H ₁₈ N ₃ O ₂ Cl
fw	528.33	543.30	450.21
cryst. color, habit	orange, prism	yellow, prism	orange, prism
cryst. dimensions (mm)	0.15 × 0.12 × 0.11	0.12 × 0.23 × 0.21	0.18 × 0.13 × 0.05
cryst. syst	orthorhombic	monoclinic	triclinic
<i>a</i> (Å)	22.613(5)	21.143(10)	8.611(1)
<i>b</i> (Å)	5.311(1)	14.237(10)	7.983(1)
<i>c</i> (Å)	18.137(5)	17.331(9)	13.890(3)
α (deg)			87.206(9)
β (deg)		99.18(3)	77.22(1)
γ (deg)			117.437(9)
<i>V</i> (Å ³)	2178.1(9)	5150(5)	844.3(3)
space group	<i>Pca</i> 2 ₁	<i>C2/c</i>	<i>P1</i>
<i>Z</i> value	4	8	2
<i>D</i> _{calc} (g/cm ³)	1.611	1.401	1.771
<i>F</i> (000)	1072.00	2432.00	452.00
μ (Mo K α)/cm ⁻¹	10.02	8.53	12.75
$2\theta_{\max}$ /°	54.9	55.0	55.0
observed reflns	20 852	18 822	8164
independent reflns	19 528	5844	3764
reflns used	19 528	5844	3764
number of variables	281	334	226
<i>R</i> ₁ [<i>I</i> > 2 σ (<i>I</i>)] ^a	0.053	0.091	0.035
<i>R</i> _w (all data) ^b	0.115	0.206	0.089

$$^a R_1 = \sum ||F_o| - |F_c|| / \sum |F_o| \text{ for } I > 2\sigma(I) \text{ data. } ^b R_w = \{ \sum w(|F_o| - |F_c|)^2 / \sum w F_o^2 \}^{1/2}; w = 1/\sigma^2(F_o) = \{ \sigma_c^2(F_o) + p^2/4F_o^2 \}^{-1}.$$

3-(*N*-2-Pyridylmethyl-*N*-2-hydroxy-5-nitrobenzylamino)ethylindole (HNO₂-iepp). To a solution of 2-hydroxy-5-nitrobenzylbromide (2.3 g, 10 mmol) and 3-(*N*-2-pyridylmethylamino)-ethylindole^{23,24} (2.6 g, 10 mmol) in THF (50 mL) was carefully added triethylamine (1.0 g, 10 mmol). The resulting solution was stirred for 3 days at room temperature and evaporated almost to dryness under a reduced pressure. The residue was purified by silica gel column chromatography to give a yellow powder. Yield: 1.95 g (48%). ¹H NMR (400 MHz, CDCl₃): δ (vs TMS) 11.04 (br, 1H), 8.59 (d, 1H), 8.04 (q, 1H), 7.93 (s, 1H), 7.63 (t, 1H), 7.33 (m, 2H), 7.20 (m, 3H), 6.94 (d, 1H), 6.80 (d, 1H), 3.99 (s, 2H), 3.90 (s, 2H), 2.98 (m, 4H).

(*N*-2-Pyridylmethyl-3-indolylethylamino)acetic Acid (Hiepc). To a solution of bromoacetic acid (2.3 g, 10 mmol) and 3-(*N*-2-pyridylmethylamino)ethylindole^{23,24} (2.6 g, 10 mmol) in ethanol (25 mL) was carefully added triethylamine (1.0 g, 10 mmol). The resulting solution was refluxed for 12 h and then evaporated almost to dryness under a reduced pressure. The residue was purified by silica gel column chromatography to give a pale-yellow powder. Yield: 2.4 g (77%). ¹H NMR (400 MHz, D₂O): δ (vs TSP) 7.98 (d, 1H), 7.50 (d, 1H), 7.25 (m, 2H), 7.17 (t, 1H), 4.44 (s, 2H), 3.94 (s, 2H), 3.52 (t, 2H), 3.21 (t, 2H).

[Pd(tbu-iepp)Cl] (1). Preparation of this complex has been reported previously.¹⁸

[Pd(MeO-iepp)Cl] (2). To a solution of HMeO-iepp (0.38 g, 1.0 mmol) in 1:1 (v/v) CH₂Cl₂/CH₃CN (20 mL) was added PdCl₂ (0.18 g, 1.0 mmol). A few drops of triethylamine were added to the resulting solution, which was stirred overnight at room temperature to give orange crystals. Anal. Calcd for **2** (C₂₄H₂₄N₃O₂ClPd): C, 54.56; H, 4.58; N, 7.95. Found: C, 54.68; H, 4.41; N, 7.89. ¹H NMR (400 MHz, DMSO-*d*₆): δ (vs TMS) 10.77 (s, 1H), 8.69 (d, 1H), 8.08 (t, 1H), 7.73 (d, 1H), 7.52 (t, 1H), 7.25 (d, 1H), 7.05 (d, 1H), 7.00 (d, 1H), 6.97 (s, 1H), 6.81 (m, 2H), 6.64 (m, 2H), 5.06 (d, 1H), 4.63 (d, 1H), 4.47 (d, 1H), 3.72 (d, 1H), 3.61 (s, 3H), 3.09 (m, 1H), 2.86 (m, 1H), 2.77 (m, 2H).

[Pd(NO₂-iepp)Cl]·0.5H₂O (3). This complex was prepared in a manner similar to that described for **2** and was given as yellow crystals. Anal. Calcd for **3** (C₂₃H₂₁N₄O₃ClPd·0.5H₂O): C, 50.16;

H, 4.22; N, 9.70. Found: C, 50.02; H, 4.01; N, 10.14. ¹H NMR (400 MHz, DMSO-*d*₆): δ (vs TMS) 10.84 (s, 1H), 8.73 (d, 1H), 8.30 (d, 1H), 8.15 (t, 1H), 7.95 (q, 1H), 7.80 (d, 1H), 7.55 (t, 1H), 7.25 (d, 1H), 7.04 (t, 1H), 6.99 (d, 1H), 6.81 (d, 1H), 6.74 (d, 1H), 4.78 (d, 1H), 4.57 (d, 1H), 4.00 (d, 1H), 3.20 (m, 1H), 2.88 (m, 2H), 2.76 (m, 1H).

[Pd(iepc)Cl] (4). To a solution of Hiepc (0.31 g, 1.0 mmol) in 1:1 (v/v) EtOH/CH₃CN (20 mL) was added PdCl₂ (0.18 g, 1.0 mmol). Triethylamine (0.1 g, 1.0 mmol) was added to the resulting solution, which was refluxed for 30 min to give yellow crystals. Anal. Calcd for **4** (C₁₈H₁₈N₃O₂ClPd): C, 48.02; H, 4.03; N, 9.33. Found: C, 48.09; H, 3.77; N, 9.32. ¹H NMR (400 MHz, DMSO-*d*₆): δ (vs TMS) 10.91 (br, 1H), 8.42 (d, 1H), 8.07 (t, 1H), 7.63 (d, 1H), 7.50 (t, 1H), 7.41 (d, 1H), 7.26 (d, 1H), 7.22 (d, 1H), 7.05 (t, 1H), 6.93 (t, 1H), 5.23 (d, 1H), 4.58 (d, 1H), 4.34 (d, 1H), 3.67 (d, 1H), 3.33 (m, 2H), 3.03 (m, 2H).

X-ray Structure Determination. The X-ray experiments were carried out on a Rigaku RAXIS imaging plate area detector with graphite monochromated Mo K α radiation ($\lambda = 0.71073$ Å). The crystal was mounted on a glass fiber. To determine the cell constants and orientation matrix, three oscillation photographs were taken for each frame with an oscillation angle of 3° and an exposure time of 3 min. Intensity data were collected by taking oscillation photographs. Refraction data were corrected for both Lorentz and polarization effects. The structures were solved by the direct method and refined anisotropically for non-hydrogen atoms by full-matrix least-squares calculations. Refinement was continued until all shifts were smaller than one-third of the standard deviations of the parameters involved. Atomic scattering factors were taken from the literature.²⁵ All hydrogen atoms were located at the calculated positions, assigned a fixed displacement, and constrained to ideal geometry with C–H = 0.95 Å and N–H = 0.90 Å. The thermal parameters of calculated hydrogen atoms were related to those of their parent atoms by $U(H) = 1.2U_{eq}(C, N)$. All the calculations were performed by using the TEXSAN crystallographic software program package from Molecular Structure Corporation.²⁶ Sum-

(25) Ibers, J. A.; Hamilton, W. C. *International Tables for X-ray Crystallography*; Kynoch: Birmingham, U. K., 1974; Vol. IV.

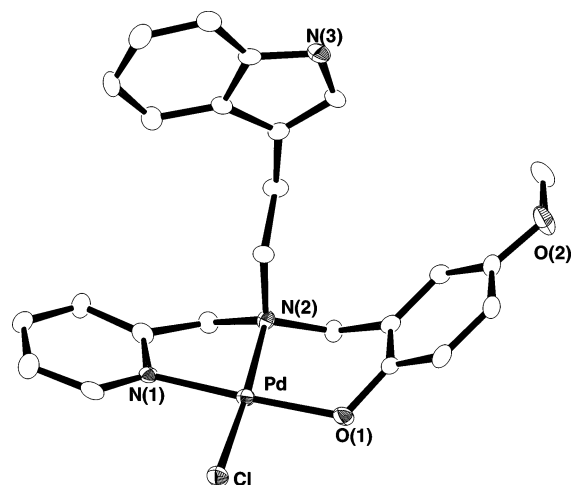


Figure 2. ORTEP view of [Pd(MeO-iepp)Cl] (**2**) drawn with the thermal ellipsoids at the 50% probability level and the atomic labeling scheme.

maries of the fundamental crystal data and experimental parameters for the structure determinations of complexes **2–4** are given in Table 1.

Spectroscopies and Kinetic Measurements. Electronic spectra were measured with a Shimadzu UV-3101PC spectrophotometer, equipped with a temperature-controlled apparatus. The temperature of the reaction solution was held constant to within ± 0.1 °C. The rate constants were determined by a least-squares analysis for complexes **1–4**. The NMR measurements were performed with a JEOL JNM-GSX-400 (400 MHz) NMR spectrometer.

Results and Discussion

Preparations and Structures of Pd(II) Complexes. HMeO-iepp and HNO₂-iepp, where H denotes a dissociable proton, reacted with PdCl₂ and triethylamine in CH₂Cl₂/CH₃CN at room temperature to give [Pd(MeO-iepp)Cl] (**2**) and [Pd(NO₂-iepp)Cl] (**3**) as red and yellow crystals, respectively. [Pd(iepc)Cl] (**4**), having a carboxylate donor, was obtained as orange crystals by the reaction in 1:1 (v/v) C₂H₅OH/CH₃CN at 80 °C. Complexes **2**, **3**, and **4** were revealed to have a mononuclear square-planar structure with a phenolate or carboxylate oxygen, an amine nitrogen, a pyridine nitrogen, and a chloride ion, as shown in Figures 2, 3, and 4, respectively. The side chain indole ring is not coordinated and is without any interactions within the complex molecules. These structures are very similar to that of complex **1**.¹⁸ The Pd–N and Pd–O bond lengths (Pd–N = 2.00–2.05; Pd–O = 1.98–2.03 Å) (Table 2) correspond well with those reported for Pd(II) complexes.^{23,27} The Pd–O bond length increased in the order **2** [1.989(2) Å] < **3** [2.006(7) Å] < **4** [2.026(2) Å] (Table 2), which is in agreement with the order of the pK_a values of the substituted phenol of the carboxylic acid of these ligands.^{28,29}

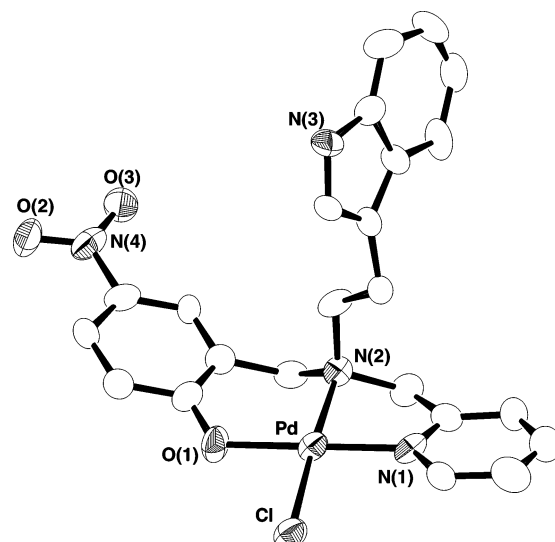


Figure 3. ORTEP view of [Pd(NO₂-iepp)Cl] (**3**) drawn with the thermal ellipsoids at the 50% probability level and the atomic labeling scheme.

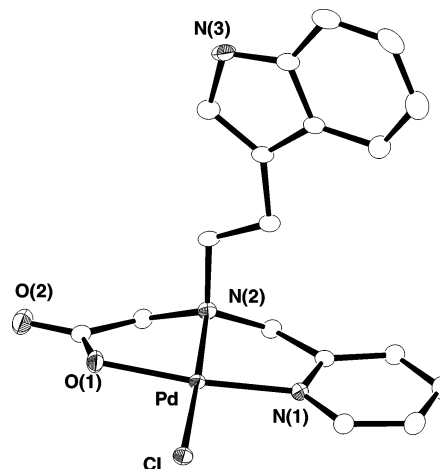


Figure 4. ORTEP view of [Pd(iepc)Cl] (**4**) drawn with the thermal ellipsoids at the 50% probability level and the atomic labeling scheme.

Table 2. Selected Bond Lengths (Å) and Angles (deg) for **2**, **3**, and **4**

	2	3	4
Bond Length (Å)			
Pd–Cl(1)	2.317(1)	2.296(3)	2.3254(6)
Pd–O(1)	1.989(2)	2.006(7)	2.026(2)
Pd–N(1)	2.019(2)	1.999(9)	2.005(2)
Pd–N(2)	2.052(3)	2.042(7)	2.020(2)
Bond Angle (deg)			
Cl(1)–Pd–O(1)	88.81(8)	86.8(2)	94.73(6)
Cl(1)–Pd–N(1)	95.16(7)	94.3(2)	97.63(7)
Cl(1)–Pd–N(2)	174.09(7)	176.7(3)	175.18(7)
O(1)–Pd–N(1)	175.93(9)	178.0(3)	167.31(8)
O(1)–Pd–N(2)	93.7(1)	96.0(3)	83.60(9)
N(1)–Pd–N(2)	82.40(9)	82.9(3)	84.29(9)

In this connection, the Pd–N(amine) bond length decreased in the order **2** [2.052(3) Å] > **3** [2.042(7) Å] > **4** [2.020(2) Å], but the trans effect in these complexes has not been observed explicitly.

Characterization of the Pd(II) Complexes. The absorption spectrum of **2** in DMF in the range 250–1000 nm exhibited peaks at 340 (ϵ = 4000) and 457 nm (ϵ = 950), the latter of which has been assigned to the phenolate-to-Pd(II) charge-transfer band (LMCT).^{18,23} While complex **3**

(26) TEXSAN, Crystal Structure Analysis Package; Molecular Structure Corporation: The Woodlands, TX, 1985 and 1999.

(27) Barnard, C. T. J.; Russel, M. J. H. In *Comprehensive Coordination Chemistry*; Wilkinson, G., Gillard, R. D., McCleverty J. A., Eds.; Pergamon: Oxford, 1987; Vol. 5, Chapter 53.

(28) Gross, K. C.; Seybold, R. G. *Int. J. Quantum Chem.* **2001**, 85, 569–579.

(29) Martell, A. E.; Smith, R. M. *Critical Stability Constants*; Plenum Press: New York, 1977; Vol. 3.

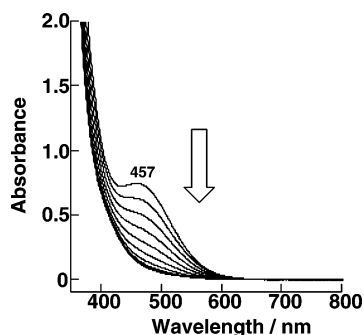


Figure 5. Absorption spectral changes of **2** with time in DMSO at 60 °C (1.0×10^{-3} M). The spectra were recorded at 30 min intervals.

with a coordinated *p*-nitrophenolate showed a strong absorption peak at 389 nm ($\epsilon = 1900$) that is assigned to the *p*-nitrophenolate $\pi-\pi^*$ transition band, the phenolate-to-Pd(II) LMCT band that was observed at 450 nm for **1**¹⁸ was not detected for **3**. The absorption spectrum of the carboxylate complex **4** showed one peak at 314 nm ($\epsilon = 2500$). The ¹H NMR chemical shifts of the indole and pyridine rings for all the complexes were very similar, and this supports that conformations of these complexes, including the side chain indole ring, are similar in solution. Since **1** had already been reported to be without stacking interactions in solution,^{18,23} the environment of the indole ring in all of the complexes is probably free from constraint and allows free rotation. These observations indicate that the side chain conformations as well as the coordination structures are maintained both in the solid state and in solution.

Formation of the Indole-Binding Pd(II) Complexes.

When the solution of **1** and **2** in DMSO or DMF was kept at 50 °C for a few days, a color change from orange to yellow was observed.¹⁸ When a solution of **2** in DMF was left to stand at 50 °C for 1 day, the LMCT band at 457 nm and the $\pi-\pi^*$ band at 340 nm gradually disappeared with the appearance of a 294 nm band ($\epsilon = 10\,000$), indicating the formation of a different complex (**2b**) containing a protonated phenol moiety¹⁸ (Figure 5), and similar spectral changes were also observed for **3** and **4**, showing that the corresponding indole-binding species were formed from these complexes. The ¹H NMR spectra of **2** in DMSO measured under different conditions indicated the conversion of **2** to **2b** at 60 °C (Figure 6); the signals of the indole C4 through C7 protons (in4–in7) shifted upfield in **2b** relative to those of **2** with chemical shift differences, $\Delta\delta = -(\delta_{2b} - \delta_2)$, of 0.02–0.67 ppm (Table 3), and the ¹H–¹H COSY spectrum revealed that **2b** lacks the indole C2 proton signal. These results indicate that the phenolato complex **2** was converted to the indole-binding complex species where Pd(II) binds with the C2 atom of the indole ring with deprotonation. Although the crystal structure of the indole-binding complex **1b** has been successfully determined,¹⁸ we could not isolate and structurally characterize the indole-binding complexes **2b**, **3b**, and **4b**. The ratio of **1** to **1b** was 1:0.3 in DMSO after 24 h at room temperature and 1:1 at 60 °C,¹⁸ while more than 90% of **2** could be converted to **2b** at 60 °C in DMSO or DMF. Complete conversion of **2** was not possible at 100 °C and higher temperatures because of the decomposition

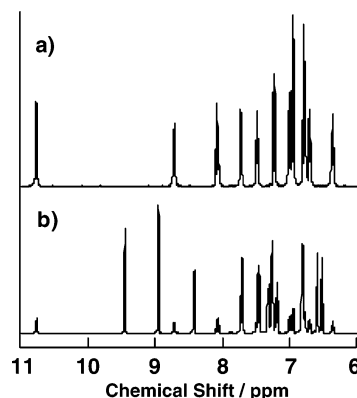


Figure 6. ¹H NMR spectra of **2** (a) in DMSO-*d*₆ and (b) heated for 24 h at 60 °C in DMSO-*d*₆; concentration, 1.0×10^{-3} M.

of **2b**. The first-order rate constant of the conversion reaction, k_{obs} , was estimated to be $1.22 \times 10^{-5} \text{ s}^{-1}$ at 60 °C in DMF for both **1** and **2**. The reaction rate was substantially dependent on the solvents, the order being DMF > DMSO, for example, $k_{\text{obs}} = 3.63 \times 10^{-6} \text{ s}^{-1}$ at 60 °C for **1** in DMSO. This tendency has been observed for the formation of other cyclopalladation complexes of our ligand series,¹⁸ but the solvent dependence of the reaction rate of cyclopalladation in general has been reported to be in the reverse order.^{30,31} During this conversion reaction, no intermediate was detected. Whereas the conversion between **1** and **1b** was reversible, **2b** in solution was not convertible and was very stable at room temperature, and after a few weeks at room temperature, it finally gave some decomposition products, which could not be isolated and characterized. On the other hand, **3** in DMF kept at 50 °C for 1 day exhibited a small color change; the *p*-nitrophenolate $\pi-\pi^*$ transition band gradually decreased, and a shoulder peak appeared at around 400 nm with isosbestic points. The k_{obs} value for the conversion of **3** to **3b** was estimated to be $3.64 \times 10^{-4} \text{ s}^{-1}$ at 60 °C, which is greater than that for **2**, although the final ratio of **3** to **3b** was 1:0.1 in DMF or DMSO from the ¹H NMR measurement. The carboxylato complex **4** showed the fastest rate of conversion with the estimated k_{obs} value of $1.07 \times 10^{-2} \text{ s}^{-1}$ at 60 °C in DMF (vide infra). The final ratio of **4** to **4b** was found to be 1:0.2 in DMF. These kinetic results may suggest that dissociation of the Pd–O bond is included in the rate-determining step. Complexes **3b** and **4b** were also stable, undergoing a slow decomposition over the course of a few months at room temperature.

The specific point on the conversion of **4** was shown by the NMR experiment. The chemical shifts of indole and pyridine protons for **4** were very different from those of **1–3**. For example, while the py6 proton signal of **1b–3b** exhibited an upfield shift relative to that of **1–3**,¹⁸ **4b** exhibited a downfield shift of the signal, which may suggest that **4b** has a different structure, such as a carboxylate-bridged dinuclear complex. In this connection, the kinetic studies indicated the

- (30) (a) Yagyu, T.; Aizawa, S.; Hatano, K.; Funahashi, S. *Chem. Lett.* **1996**, 1107–1108. (b) Yagyu, T.; Aizawa, S.; Funahashi, S. *Bull. Chem. Soc. Jpn.* **1998**, *71*, 619–629. (c) Yagyu, T.; Iwatsuki, S.; Aizawa, S.; Funahashi, S. *Bull. Chem. Soc. Jpn.* **1998**, *71*, 1857–1862.
(31) Ryabov, A. D.; Sakodinskaya, I. K.; Yatsimirsky, A. K. *J. Chem. Soc., Dalton Trans.* **1985**, 2629–2638.

Table 3. ^1H NMR Chemical Shifts (δ/ppm) and Upfield Shifts ($\Delta\delta$)^a of Pyridine and Indole Proton Signals for Pd(II) Complexes in DMSO-*d*₆

	δ ($\Delta\delta$)/ppm							
	tbu-iepp (1)	1b	MeO-iepp (2)	2b	NO ₂ -iepp (3)	3b	iepc (4)	4b
py3	7.77	7.16 (+0.61)	7.73	7.26 (+0.37)	7.76	7.26 (+0.50)	7.64	7.69 (−0.05)
py4	8.11	7.65 (+0.46)	8.08	7.72 (+0.36)	8.13	7.75 (+0.38)	8.08	8.05 (+0.03)
py5	7.52	7.15 (+0.37)	7.52	7.21 (+0.31)	7.53	7.20 (+0.33)	7.51	7.58 (−0.07)
py6	8.69	8.44 (+0.25)	8.69	8.47 (+0.22)	8.73	8.40 (+0.33)	8.43	8.79 (−0.26)
in1	10.74	8.34 (+2.40)	10.77	9.34 (+1.43)	10.82	9.50 (+1.32)	10.92	9.36 (+1.43)
in2	6.88		6.81		7.03		7.26	
in4	7.22	7.36 (−0.14)	7.25	7.34 (−0.09)	7.20	7.34 (−0.14)	7.42	7.28 (+0.14)
in5	6.72	6.83 (−0.11)	6.66	6.83 (−0.17)	6.79	6.83 (−0.04)	6.94	6.80 (+0.14)
in6	6.96	6.83 (+0.13)	6.81	6.83 (−0.02)	6.98	6.83 (+0.15)	7.05	6.80 (+0.15)
in7	6.72	7.29 (−0.57)	6.61	7.28 (−0.67)	6.74	7.30 (−0.56)	7.32	7.24 (+0.08)

^a $\Delta\delta = -(\delta_b - \delta_a)$, where δ_a and δ_b refer to the shifts for the O-donor complex and the corresponding indole-binding complex, respectively.

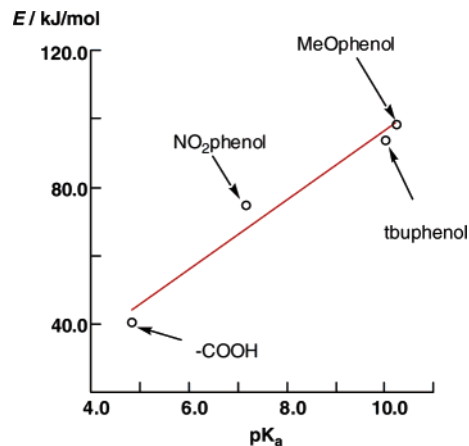
Table 4. Activation Parameters and Rate Constants at 60 °C, k^{333} , for Conversion between the O-Donor Complexes and Indole-Binding Complexes in DMF^a

	$\Delta H^\ddagger/\text{kJ mol}^{-1}$	$\Delta S^\ddagger/\text{J K}^{-1} \text{mol}^{-1}$	$10^4 k^{333}/\text{s}^{-1}$
tbu-iepp(1)	92 ± 4	−64 ± 10	0.122
MeO-iepp(2)	96 ± 2	−51 ± 6	0.122
NO ₂ -iepp(3)	72 ± 1	−94 ± 3	3.64
iepc (4)	38 ± 2	−170 ± 6	107

^a Determined by the dependence of k_{obs} on temperature (see ref 33).

presence of two components, the first one showing the first-order reaction and the second one showing the reaction of an unidentified order. From these results, the first component of the reaction of **4** was assigned to the formation of the mononuclear indole-binding species and the second one to the conversion to a dinuclear complex or an intermolecularly interacting species. We, therefore, adopted the first component value as the rate constant for the formation of **4b**.

Relation between Activation Energy and Oxygen Donor Properties in the Structural Conversion. The k_{obs} values of the above conversion reaction followed the order of the acidity of the oxygen donor, *p*-methoxyphenol < *p*-nitrophenol < carboxylic acid.^{28,29} The values for all the complexes were dependent on the reaction temperature and increased with the temperature. The activation parameters for the conversion were determined, as listed in Table 4, according to the theory of transition state by linear least-squares fitting (see Supporting Information).³³ The plot of the activation energy E versus the pK_a value of the ligand OH group (Figure 7) clearly indicates that the energy barrier of the conversion is correlated with the oxygen donor ability and, hence, with the Pd–O bond strength, the order being MeO–phenolate > NO₂–phenolate > COO[−]. It is generally agreed that cyclopalladation reactions of aryl compounds

**Figure 7.** Activation energies as a function of the pK_a values of the ligand OH groups.

proceed by an electrophilic substitution mechanism involving the rate-determining step in such processes as C–H bond cleavage, which is normally regarded as an irreversible process.^{32,34} The rate-determining step of our conversion may involve Pd–O bond cleavage in addition to the C–H bond cleavage process. On the other hand, while the activation parameters for **1** and **2** were comparable with and those for **3** were slightly smaller than the other values reported for cyclopalladation,³⁰ complex **4** exhibited a small activation enthalpy (ΔH^\ddagger) and a large negative entropy (ΔS^\ddagger) value. However, the activation parameters in Table 4 are correlated with each other, suggesting a similar mechanism of cyclopalladation in our series of Pd(II) complexes.

Effect of Addition of Acids and Bases. The rates of conversion from the phenolato complexes **2**, **3**, and **4** to the indole-binding ones were temperature-dependent, whereas the ratio of the phenolato complex to the indole-binding complex was temperature-independent in the range 40–80 °C. For example, the ratio of **4** to **4b** was estimated to be 1:0.2 from the ^1H NMR experiment in this temperature range. The addition of a few equivalents of benzoic acid to the solutions of **3** and **4** in DMSO or DMF did not affect the ratio, and the addition of 1 equiv of $\text{CF}_3\text{SO}_3\text{H}$ to the solutions of the phenolato complexes in DMSO gave some decomposition products. On the other hand, the addition of triethylamine changed the ratio: 4 equiv of triethylamine

(32) (a) Parshall, G. W. *Acc. Chem. Res.* **1970**, *3*, 139–144. (b) Ryabov, A. D. *Chem. Rev.* **1990**, *90*, 403–424. (c) Beller, M.; Riermeier, T. H.; Haber, S.; Kleiner, H.-J.; Herrmann, W. A. *Chem. Ber.* **1996**, *129*, 1259–1264.

(33) If the reactions in this study proceed via an intramolecular reversible process, k_{obs} should be expressed by the rate constants for the formation of the indole-binding complex (k_f) and the phenolato complex (k_b) as follows: $k_{\text{obs}} = k_f + k_b$. The equilibrium constant (K) for each system can be estimated from the final ratio of the indole-binding complex to the phenolato complex, $K = k_f/k_b$. However, the subsequent side (decomposition) reactions in the present systems gave rise to large errors in the estimation of k_f and k_b and prevented the determination of the detailed final ratios (see text). Therefore, only the temperature dependence of k_{obs} was measured and used for the calculation of the activation parameters.

(34) Gómez, M.; Granell, J.; Martínez, M. *Eur. J. Inorg. Chem.* **2000**, 217–224.

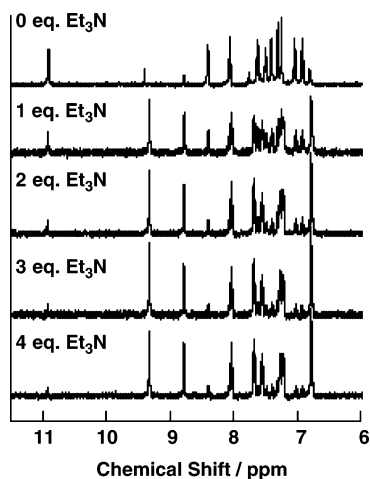
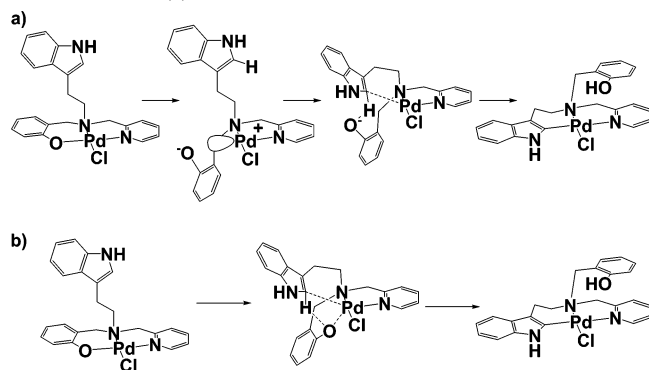


Figure 8. ^1H NMR spectral changes of **4** in $\text{DMSO}-d_6$ with the addition of triethylamine at 60°C ; concentration, 1.0×10^{-3} M.

Scheme 2. Proposed Mechanisms of Formation of the Indole-Binding Complex: (a) Mechanism via 14-Electron Three-Coordinate Intermediate and (b) Mechanism via Five-Coordinate Intermediate



added to the solution of **4** in DMSO at 70°C gave **4b** in more than 90% yield, as seen from the ^1H NMR spectral changes (Figure 8). A similar tendency was also observed for **3** in DMSO , where the yield of the indole-binding complex **3b** was increased 2 times by 5 equiv of triethylamine at 70°C . Accordingly, a more basic condition is more favorable for the formation of the indole-binding complex³⁰ and, thus, the cyclopalladation.

Conversion Mechanism. Recently, we reported that the phenol OH group takes part in the process of the structural conversion between **1** and **1b**, where the phenolate oxygen abstracts the indole C2 proton to form **1b**.¹⁸ This result is in agreement with the present result on the ratio of the phenolato complex to the indole-binding complex, the conversion ratio being lower for **3** and **4** containing a weak proton acceptor.^{28,29} In contrast, the reaction rates for **3** and **4** were greater than those for **1** and **2** because of facile Pd–O bond cleavage. The observed conversion may be interpreted by the proposed cyclopalladation mechanisms shown in Scheme 2. One of them involves a three-coordinate 14-electron intermediate (Scheme 2a),^{31,32,34–36} which explains the observation that

the cyclopalladation reaction is inhibited by excessive amounts of additional ligands such as triphenylphosphine (PPh_3).³⁴ According to the other mechanism (Scheme 2b), cyclopalladation proceeds by the concerted mechanism via a five-coordinate intermediate.³⁰ If the former mechanism is applied to our system, Pd–O bond cleavage as the first step may be favored by the existence of protons. In the present systems, however, the addition of benzoic acid to the phenolato complexes in DMSO or DMF had only a slight effect on the conversion, and an excess of PPh_3 did not replace the coordinated phenolate moiety; the indole-binding species was formed irrespective of these conditions. On the basis of this observation and considering that the reaction was accompanied by a large negative entropy change as compared with the other cyclopalladation,³⁰ we may exclude the three-coordinate 14-electron intermediate. Since the rate-determining step of both mechanisms has been proposed to be the C–H bond cleavage,^{30–32,34–36} the existence of protons is considered to be unfavorable for the cyclopalladation.

It is generally agreed that cyclopalladation reactions of aryl compounds proceed by an electrophilic substitution by $\text{Pd}(\text{II})$ ions. The electrophilicity of the $\text{Pd}(\text{II})$ center to the indole moiety should increase with the decreasing $\text{p}K_a$ values of the ligand OH group, and our experiments have shown that the reaction rates are in the order $2 < 1 < 3 < 4$, which is in agreement with the decreasing order of the $\text{p}K_a$ values of the corresponding ligands. Despite the lack of further experimental results on the activated intermediate, we may suggest that the intermediate of the conversion reaction is associated with the O-donor properties of the ligands, and all of our results are consistent with those hitherto reported.^{30–32,34–36}

Conclusion. We prepared and characterized the $\text{Pd}(\text{II})$ complexes of a series of new tripod-like 2N1O-donor ligands containing an oxygen donor with various substituents and a pendent indolyethyl moiety. In the temperature range of 40 – 80°C , all the $\text{Pd}(\text{II})$ complexes yielded the corresponding indole-binding $\text{Pd}(\text{II})$ species, whose formation rate constants and activation parameters have been determined. The relationship between the structures of the complexes and the activation parameters indicated that the formation rate of the indole-binding $\text{Pd}(\text{II})$ species depends on the O-donor properties, the complexes of the ligands with a lower ligand OH $\text{p}K_a$ value exhibiting a faster conversion to the indole-binding species in the order $2 < 3 < 4$. On the other hand, the formation ratio of the indole-binding complex to the O-donor complex was higher for the complexes of the ligands with a higher $\text{p}K_a$ value in the order $2 > 3 > 4$. The addition of a base enhanced the formation of the indole-binding complex, which indicates that basic conditions are favorable for the present cyclopalladation. Although no reaction intermediate was detected in the present study, the O-donor to C-donor conversion reaction may be explained by a mechanism involving a five-coordinate intermediate, which is not in conflict with the proposals that have been reported.^{30–32,34–36} The present findings may add to our knowledge of the properties of the indole ring under various conditions.

(35) Deeming, A. J.; Rothwell, I. P. *Pure. Appl. Chem.* **1980**, *52*, 649–655.

(36) (a) Thummel, R. P.; Jahng, Y. J. *J. Org. Chem.* **1987**, *52*, 73–78. (b) Gómez, M.; Granell, J.; Martínez, M. *Organometallics* **1997**, *16*, 2539–2546.

Acknowledgment. We gratefully acknowledge the support of this work by a Grant-in-Aid for Scientific Research (Grant 17750055 to Y.S. and Grant 16350036 to O.Y.) and the “Nanotechnology Support Project” of the Ministry of Education, Culture, Sports, Science and Technology of Japan.

Supporting Information Available: The X-ray crystallographic data (CIF) for complexes **2**, **3**, and **4** and ¹H NMR spectra (PDF) showing the interconversion. This material is available free of charge via the Internet at <http://pubs.acs.org>.

IC0504801